Rapid Photodynamics of Vitamin B_6 Coenzyme Pyridoxal 5′-Phosphate and Its Schiff Bases in Solution

Melissa P. Hill, Elizabeth C. Carroll, Michael D. Toney, and Delmar S. Larsen*

Department of Chemistry, University of California, Davis, One Shields Avenue, Davis, California 95616

Received: December 13, 2007; In Final Form: February 4, 2008

The active form of vitamin B_6, pyridoxal 5′-phosphate (PLP), is an important cofactor for numerous enzymes in amine and amino acid metabolism. Presented here is the first femtosecond transient absorption study of free PLP and two Schiff bases, PLP-valine and PLP-α-aminoisobutyric acid (AIB), in solution. Photoexcitation of free PLP leads to efficient triplet formation with an internal conversion rate that increases with increasing pH. The measured excited-state kinetics of the PLP-valine Schiff base exhibits a dramatic deuterium dependence as a result of excited-state proton transfer (ESPT) of the Cα hydrogen in the amino acid substrate. This is consistent with formation of the key reaction carbanionic intermediate (quinonoid), which is resonance stabilized by the electron-deficient, conjugated π system of the Schiff base/pyridine ring. The transient absorption signals of the PLP-Schiff base with α-methylalanine (2-aminoisobutyric acid), which does not have a Cα proton, lack an observable deuterium effect, verifying ESPT formation of the quinonoid intermediate. In contrast to previous studies, no dependence on the excitation wavelength of the femtosecond kinetics is observed with PLP or PLP-valine, which suggests that a rapid (<250 fs) tautomerization occurs between the enolimine (absorbing at 330 nm) and ketoenamine (absorbing at 410 nm) tautomers in solution.

1. Introduction

Pyridoxal 5′-phosphate (PLP), one form of vitamin B_6, is a chromophoric coenzyme required by more than 4% of known enzymes. These enzymes are central to numerous metabolic pathways involving nitrogen and catalyze a wide variety of chemistries, including transamination, decarboxylation, racemization, aldol cleavage, and additional reaction types.[1−3] The catalytic activity of PLP is based on formation of a carbanion after Schiff base (imine) formation with an amine-containing substrate. Carbanion stabilization by PLP is attributed to the extended π conjugation in the Schiff base/pyridine ring system (Figure 1). The strong electron-withdrawing ability of the protonated Schiff base and the protonated pyridine ring strongly polarizes covalently bound substrates through hyperconjugation, providing both ground-state destabilization and transition-state and product stabilization.

Although the activity of PLP-dependent enzymes does not intrinsically require the input of light, Fraikin et al. reported that near-UV (337 nm) excitation increases catalytic activity in 5′-hydroxytryptophan decarboxylase, a PLP-dependent enzyme that catalyzes the decarboxylation of 5′-hydroxytryptophan to serotonin.[4] Complementing this observation, Cornish and Ledbetter demonstrated that laser excitation of PLP in aspartate aminotransferase generates the central carbanionic (quinonoid) intermediate.[5] Both observations illustrate the potential of using optical spectroscopic techniques for characterizing protein dynamics that are central to the reaction mechanism of the enzyme−substrate complexes.

Modern ultrafast laser systems offer exceptional time resolution for such spectroscopic studies and are unique in their ability to generate rapidly intermediates of reaction mechanisms because of their high intensity. The approach presented here is analogous to previous light-induced ligand dissociation studies in myoglobin[6] and bond rupture dynamics in vitamin B_{12}.[7] However, the focus of our investigations is the protein cleavage of the more stable C−H and C−CO_2 bonds. Despite its broad utility, no femtosecond time-resolved studies have been reported on PLP, its derivatives in solution or bound in enzyme environments.

In the absence of substrate molecules, all PLP-dependent enzymes covalently bind PLP in the active site as an "internal" Schiff base with a conserved lysine residue.[3] The binding of an amine-containing substrate molecule to the enzyme results in the formation of an "external" Schiff base that, in the course of catalysis, loses an electrophile (e.g., H^+ or CO_2) to form a high-energy carbanion intermediate, termed the "quinonoid", central to all PLP-catalyzed mechanisms.[1,3] Each tautomer and intermediate of a PLP-Schiff base has a distinct spectroscopic signature enabling isolated PLP and PLP-Schiff bases to be used as model compounds in numerous chemical and spectroscopic studies to gain insight into the mechanisms involved in PLP enzymatic catalysis.[1,3,5,8−14] Here, we present the first femtosecond investigation of the photodynamics for free PLP and its Schiff base with valine and α-aminoisobutyric acid (AIB) in aqueous solution (Figure 1). The signals measured for the PLP Schiff base with α-methylated amino acid, AIB, are compared to those for the PLP-valine Schiff base since AIB lacks an α-proton whose cleavage is necessary for the excited-state proton transfer (ESPT) formation of the quinonoid intermediate in the transamination (Figure 2).

2. Experimental Methods

The dispersed-probe transient absorption spectrometer is based on an amplified Ti:sapphire laser system (Spectra Physics Spitfire Pro and Tsunami) producing 2.25-mJ pulses at 800 nm with 40-fs (fwhm) duration at a 1-kHz repetition rate. A more

* Corresponding author. Phone: 530-754-9075. Fax: 530-752-8995. E-mail: dlarsen@ucdavis.edu.

10.1021/jp7117345 CCC: $40.75
Published on Web 04/17/2008

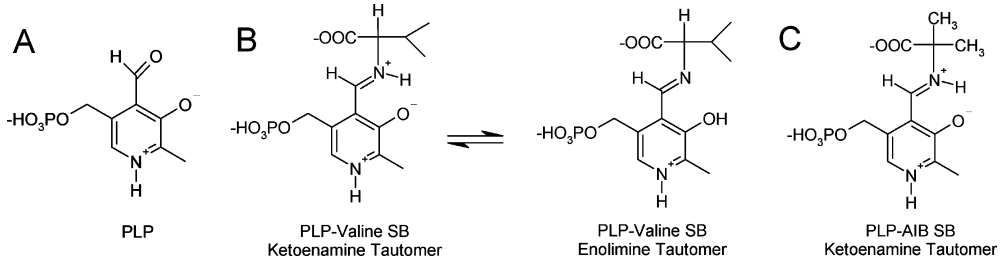

Figure 1. (A) Structure of PLP at pH 7.0. (B) Structure of the ketoenamine and enolimine tautomers for the PLP-valine Schiff base (SB). (C) Structure of the ketoenamine PLP-AIB Schiff base.

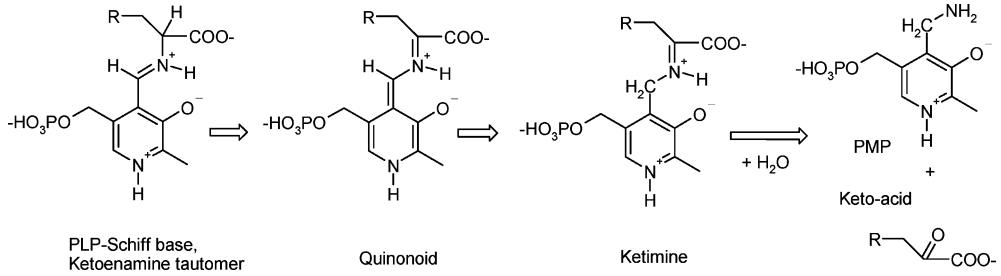

Figure 2. Transamination half-reaction scheme involving ketoenamine tautomer of a generic PLP Schiff base (SB) where R is the side chain of the amino acid.

detailed description of this setup can be found elsewhere;[15] we highlight the relevant experimental details here. The experimental setup includes the generation of a femtosecond white-light continuum (320−650 nm) that acts as the probe pulse and an excitation wavelength centered at either 350 or 400 nm that acts as pump pulses. The 800-nm fundamental pulse from the laser was frequency doubled in a 500-μm β-barium borate crystal to produce 4-mW, 50-fs pulses at 400 nm. Excitation light (350 nm) was generated by sum frequency mixing 620-nm light from a home-built non-collinear optical parametric amplifier with the fundamental 800-nm light. The polarization of the probe light was set at magic angle (54.7°) with respect to the pump polarization.

Interrogated samples were flowed through a home-built quartz cuvette constructed with 150-μm-thick quartz windows to reduce coherent artifacts and to improve time resolution.[16] Path lengths were either 0.8 mm (for 1 mM) or 0.3 mm (for 5 mM) to generate an OD of 0.8 per sample (at max wavelength). Instrument response functions of approximately 70 fs (400-nm pump) and 250 fs (350-nm pump) were determined by cross-correlation of the pump and probe pulses measured by two-photon absorption in buffer solution.

PLP (Acros), L-valine (Fisher), α-aminoisobutyric acid (Sigma), HEPES (Sigma), and CAPS (Sigma) were obtained commercially in the highest quality available and used without further purification. HEPES (0.1 M) and CAPS (0.1 M) buffers were used in the appropriate pH ranges adjusted with either 1 M NaOH or 1 M HCl. For preparation of Schiff base samples, PLP (1.5×10^{-3} M) was reacted with an excess of valine (0.1 M) in indicated solvents. All PLP-valine samples were purged with nitrogen gas for approximately 3 h before irradiation to rid the sample of dissolved oxygen and ensure photostability.[8,17−19]

3. Results and Discussion

3.1. Free PLP in Solution. The static absorption spectrum of free PLP exhibits different bands depending on the pH of the solvent (Supporting Information, Figure S1), corresponding to the protonation at four sites with well-known pK_a values: pK_1 = 8.69 (protonation of the pyridine nitrogen), pK_2 = 6.1 (first protonation of the phosphate group), pK_3 = 3.7 (protonation of the 3′-hydroxyl group), and pK_4 ≈ 2.5 (second protonation of the phosphate group).[1,3,20] At pH 7, PLP in solution exhibits an absorption spectrum with a peak at 388 nm and a distinct shoulder at ∼330 nm; its fluorescence spectrum shows a maximum at 500 nm. With increasing pH, the absorption maximum red-shifts slightly and the shoulder at 330 nm disappears; accordingly, the fluorescence maximum is at 540 nm. At acidic pH, the absorbance of PLP peaks at 294 nm. The corresponding fluorescence data show a larger Stokes shift for free PLP at pH 10 vs pH 7, suggesting greater charge rearrangement in the excited state when the pyridine nitrogen is deprotonated. Free PLP exists in both aldehyde and hydrated forms; ∼30% of PLP is hydrated at pH 7.0 as either an uncharged tautomer or a dipolar ion.[1,3,10] Hence, three different free PLP populations coexist in solution. Fortunately, only the aldehyde form absorbs at 400 nm and therefore can be selectively excited and probed in our measurements.

The transient absorption signals of free PLP excited at 400 nm in water at pH 7.0 exhibit complex dynamics extending over multiple timescales from sub-100 fs to 8 ns (Figure 3). Three strongly overlapping contributions can be clearly identified: (1) a ground-state bleach at 400 nm, (2) a stimulated emission band at 500 nm, and (3) excited-state absorption (ESA) bands at 450 nm and below 350 nm. The signals at later times (up to 8 ns) do not return to zero, indicating the formation of a primary photoproduct. Multidimensional global fitting[21,22] was used to interpret the experimental data within a postulated model that connects the observed populations with distinct spectral and/or temporal characteristics. For PLP in H_2O at pH 7.0, four populations are identified with differing species associated difference spectra (SADS) using the branched model shown in Figure 4. The reconstructed SADS exhibit stimulated emission bands for three excited-state populations, corresponding to the fluorescence spectrum (Supporting Information, Figure S1). Time constants were determined for each transition between states corresponding to the excited-state connectivity scheme in Figure 4C (Table 1).

The stimulated emission band (Figure 4B: solid to dashed SADS) of the initial subpicosecond transient spectrum rapidly red-shifts and is a feature attributable to solvation dynamics

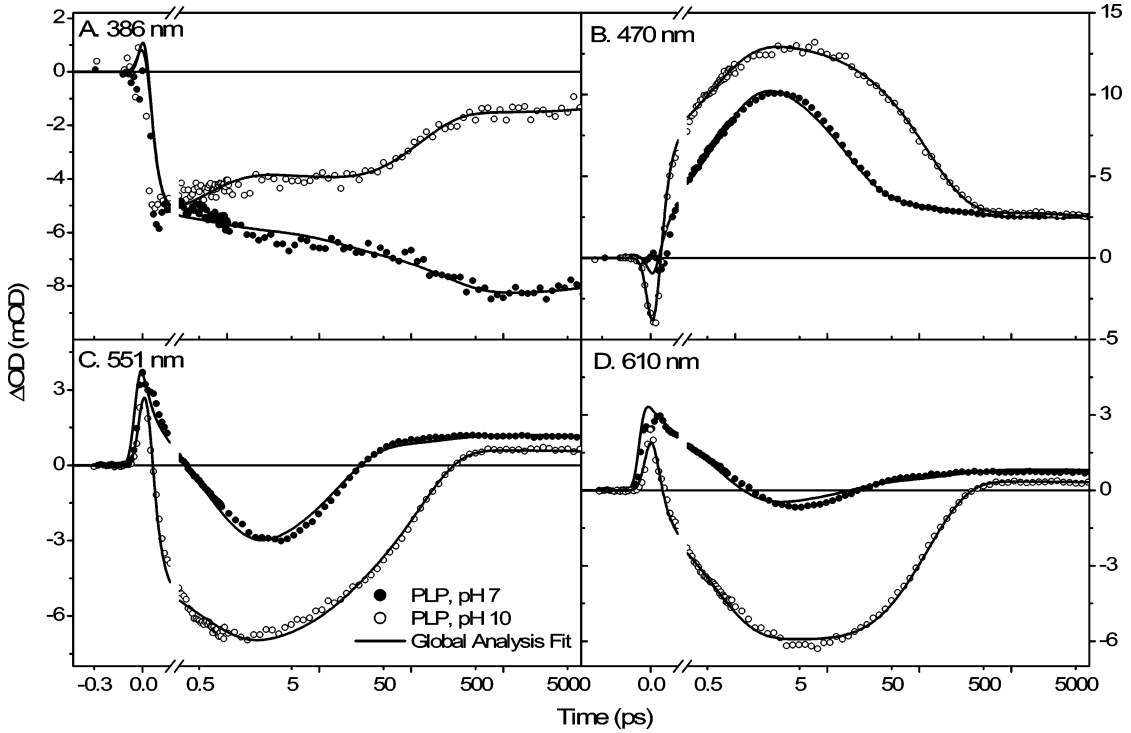

Figure 3. Kinetic traces of PLP in H_2O at pH 7.0 (●) and at pH 10.0 (○) with global analysis fit (—) at (A) 386, (B) 470, (C) 551, and (D) 610 nm.

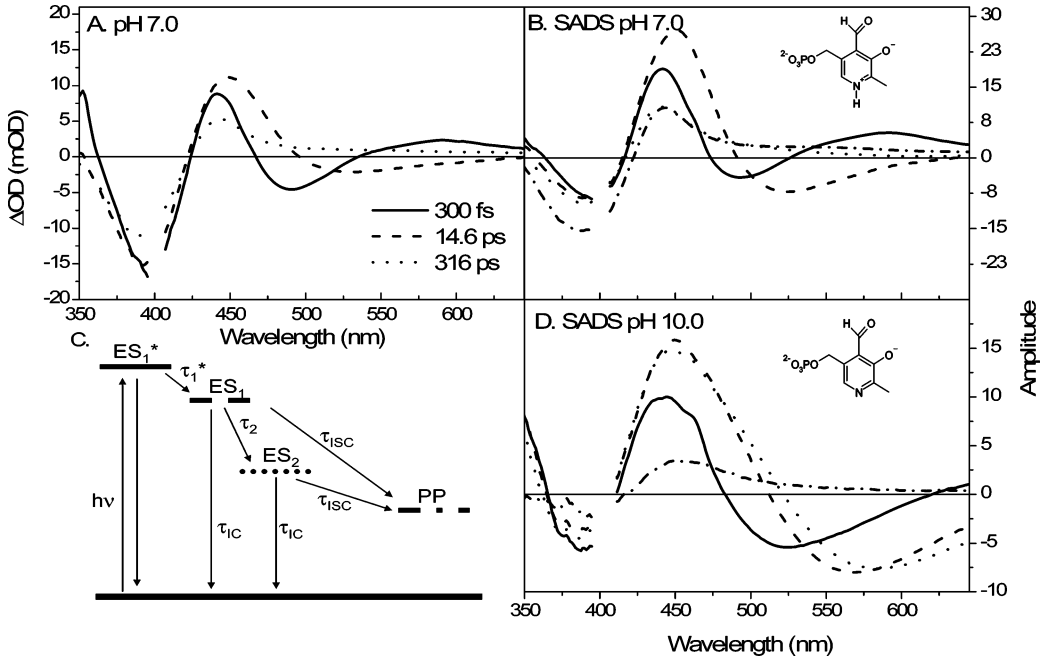

Figure 4. Transient absorption data and SADS of free PLP in H_2O. (A) Transient spectra at pH 7.0 with time points in inset. (B, D) SADS of free PLP in H_2O at (B) pH 7.0 and (D) pH 10.0 with associated excited states (ES): ES_1* (—), ES_1 (— — —), ES_2 (···), and photoproduct (PP) (— · —), time constants presented in Table 1. (C) Proposed kinetic model for free PLP. * = Solvation dynamics.

due to intermolecular rearrangements of the surrounding H_2O molecules induced by the changing electric field of PLP. Similar solvation time scales have been observed for other molecules in water,[23,24] and the interpretation of solvation dynamics is corroborated by slower red-shifting dynamics observed in transient signals for free PLP in a more viscous glycerol solution (data not shown). The second and third time constants characterize the excited-state lifetime dynamics that are modulated by quenching processes such as photoinduced reaction dynamics, internal conversion to the ground electronic state, and intersystem crossing as discussed below.

The nondecaying signal observed at long time scales (Figure 4B: dash−dot) peaks at 450 nm and exhibits a weak long-wavelength tail. This spectrum is assigned to an initial photoproduct based on its similarity to the previously characterized triplet spectrum.[1,3,17,25] Intersystem crossing yields have not been reported for this system, and fluorescence quantum yields for all ionic forms of PLP have previously been reported as less than 1%.[1] The kinetics in Figure 4 suggests a high triplet yield for free PLP. Because the bleach, which indicates the number of photoexcited PLP molecules, is obscured by the overlapping ESA at early times, direct determination of the triplet yield from

TABLE 1: Associated Excited State Lifetimes (τ) Determined by Global Analysis with Samples Excited at 400 nm[a]

sample	solvent	τ_1[b]	τ_2	τ_{IC}	τ_{ISC}	τ_{PP}
PLP	H_2O (pH 7.0)	602 fs	2.82 ps	19 ps	150 ps	∞
	H_2O (pH 10.0)	420 fs	3.02 ps	120 ps	150 ps	∞
		τ_1[b]	τ_2	τ_3		τ_{PP}
PLP-valine	H_2O (pH 7.0)	1.16 ps	63.8 ps	1.03 ns		∞
	D_2O (pD 7.0)	1.67 ps	53.3 ps	1.47 ns		∞

[a] Each τ represents the length of time the designated state lives. For example, τ_2 demonstrates the time scale by which ES_2 decays; see the corresponding connectivity schemes in Figure 5C (PLP) or 6A (PLP-valine). τ_{PP} persists throughout the duration of the experiment and is so designated with ∞ (>8 ns). [b] Denotes solvation dynamics.

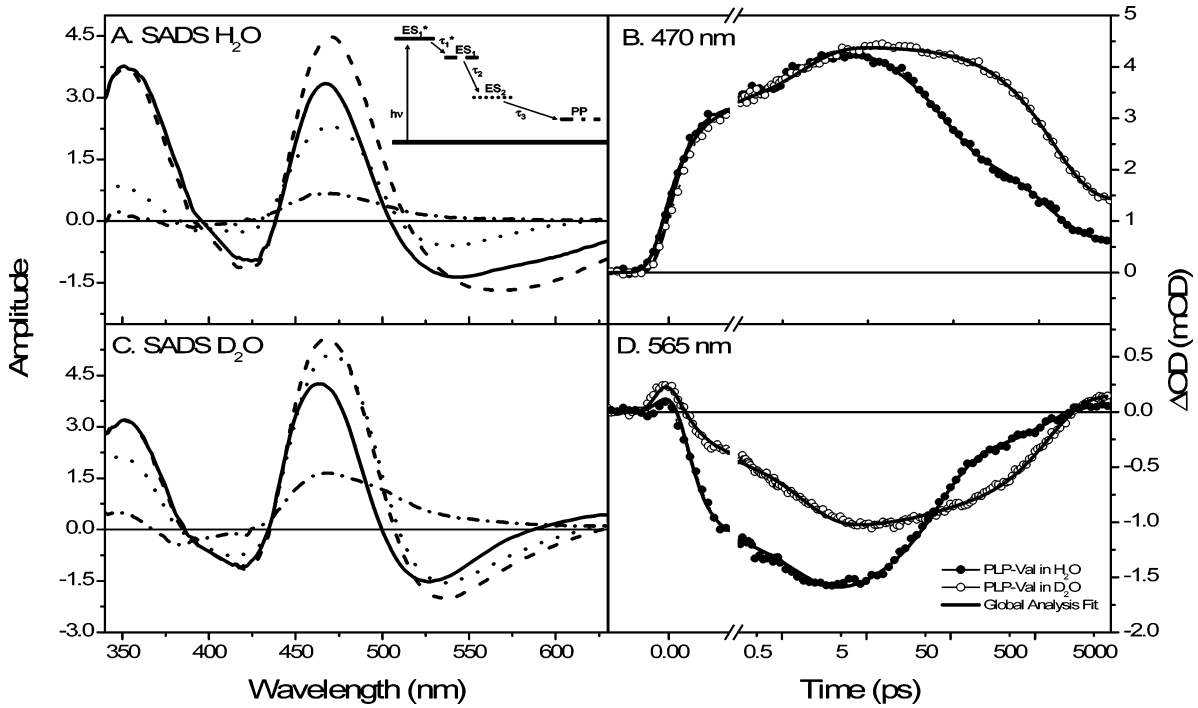

Figure 5. Data and fit of PLP-valine Schiff base. (A, C) SADS for PLP-valine Schiff base in (A) pH 7.0 H_2O and in (C) pD 7.0 D_2O with associated excited states (ES), ES_1* (—), ES_1 (— — —), ES_2 (···), and photoproduct (PP) (— · —) with inset of proposed sequential model. (B, D) Kinetic trace comparison between PLP-valine in pH 7.0 H_2O (●) and pD 7.0 D_2O (○) with global analysis fit (—) at (B) 470 nm and (D) 565 nm. * = Solvation dynamics.

these data alone is difficult. However, we can identify an upper bound of 60% since the bleach decreases by less than half over the course of the experiment, indicating the excited population did not return to the PLP ground state within 7 ns (Figure 4A). The third and fourth SADS are strikingly similar, suggesting relaxation in the triplet manifold occurs.

A distinct, stable photoproduct absorbing at ~300 nm is observed in the static absorbance spectra of the sample after irradiation, which demonstrates eventual photodegradation of PLP molecules (not shown). It is unclear if the final photoproduct is formed from the singlet excited state in parallel with intersystem crossing, or if the photoproduct is generated from the triplet state. Experiments that directly probe the 300-nm spectral region after excitation will shed light on this question and are currently in progress.

When the solvent pH is increased from 7 to 10, PLP loses its pyridine proton and exhibits differing transient absorption signals. Free PLP at pH 10 demonstrates slower dynamics (Figure 3) along with a slight red-shifting in the stimulated emission (Figure 4) that is due to the variation in the internal conversion rate with changing pH (Table 1).[1,3] This is similar to other chromophoric systems exhibiting protonation-dependent intersystem crossing rates. Analysis of the pH 10 data with the same connectivity model used for pH 7.0 data confirms these different time scales (Table 1).

Although a clear protonation dependence is observed in the photodynamics of free PLP (pH 7 vs pH 10), it is unclear from these data alone whether PLP exhibits an (ESPT) induced by the absorption of light. To determine this, we tested for a kinetic isotope effect by comparing the transient time scales for PLP in H_2O and D_2O at pH/pD 7. The resulting transient absorption signals are nearly identical for both solvents (data not shown), indicating that ESPT does not occur in free PLP.

3.2. PLP Schiff Bases in Solution. In PLP-dependent enzymes, the PLP cofactor exists in a Schiff base with a conserved lysine residue. The catalytic activity of the protein is dependent on the ability of PLP to form Schiff bases with amine and amino acid substrates, which can exist in two tautomeric forms: ketoenamine and enolimine (Figure 1). The ketoenamine tautomer (3′ hydroxyl unprotonated with the Schiff base nitrogen protonated) is the predominant form in water and has an absorption spectrum that peaks at 280 and 413 nm (Supporting Information, Figure S1). The alternate enolimine form (unprotonated Schiff base nitrogen and protonated 3′ hydroxyl) is favored in low dielectric constant solvents and absorbs predominantly at 330 nm.[3] We contrasted the PLP-valine Schiff base dynamics in solution with the free PLP chromophore dynamics as a model of catalytically relevant Schiff bases.

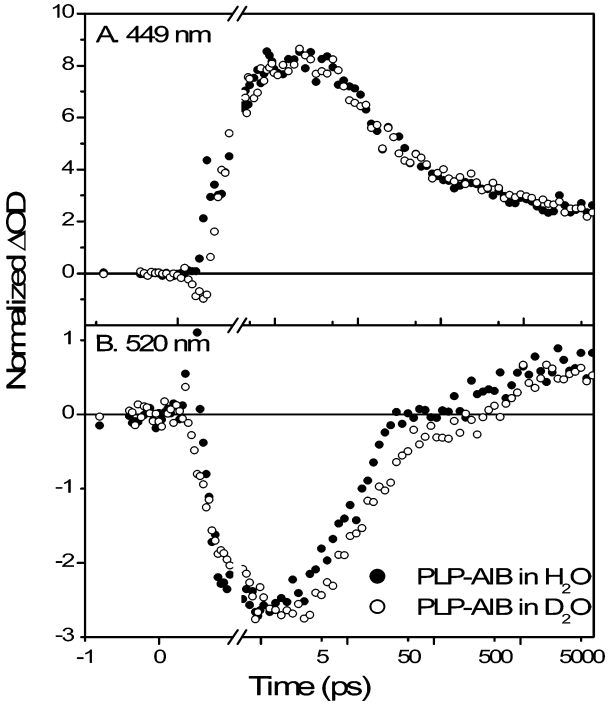

Figure 6. Kinetic traces demonstrating the lack of D_2O dependence of PLP-AIB at (A) 449 nm and (B) 520 nm in pH 7.0 H_2O (●) and pD 7.0 D_2O (○). Traces normalized to H_2O sample.

The transient absorption signals of PLP-valine in pH 7 (Figure 5), excited at 400 nm, resemble those measured for free PLP, except for two key differences: (1) the transient spectra are red-shifted because of the extension of the conjugated electrons into the Schiff base linkage and (2) the evolution time scales are distinctly slower and extend to nanoseconds. Through global analysis, we identified four sequential populations (Figure 5A and Table 1). As with free PLP, the Schiff base exhibits subpicosecond solvation dynamics and forms a primary photoproduct that exists on longer time scales than probed here (~8 ns). The static absorbance spectra taken after irradiation again show formation of permanent photoproducts, this time with a max absorption at 327 nm.

Although various explanations for the origin of the transient Schiff base absorption peak at 470 nm are possible, photoirradiation experiments consistently produce a final photoproduct with a spectrum that strongly resembles the 327-nm absorbance spectrum of pyridoxamine 5′-phosphate (PMP). PMP is formed from transamination of PLP and an amino acid (Figure 2), and its observation here implies that the transient signals mirror the initial events of the formation of the intermediates in that reaction. Transamination of PLP proceeds by initial removal of the Cα−H proton to give the carbanionic quinonoid intermediate, followed by protonation at C4′ to give the ketimine intermediate. Ketimine hydrolysis gives PMP and the α-keto acid (Figure 2). The primary photoproduct transient spectrum peaking at 470 nm is consistent with quinonoid intermediate absorbance.[5,12] Although similar to the triplet spectrum ascribed to free PLP, slower quenching dynamics in the Schiff base samples indicates a significantly slower rate of intersystem crossing and, hence, small triplet yield. Therefore, the primary photoproduct is assigned to the carbanionic quinonoid intermediate. An alternative interpretation of the 470-nm absorption peak is a back-transfer of the excited hydroxyl proton from the imine nitrogen occurring within 10 ns,[27] a very slow rate of proton transfer on the time scale of this study.

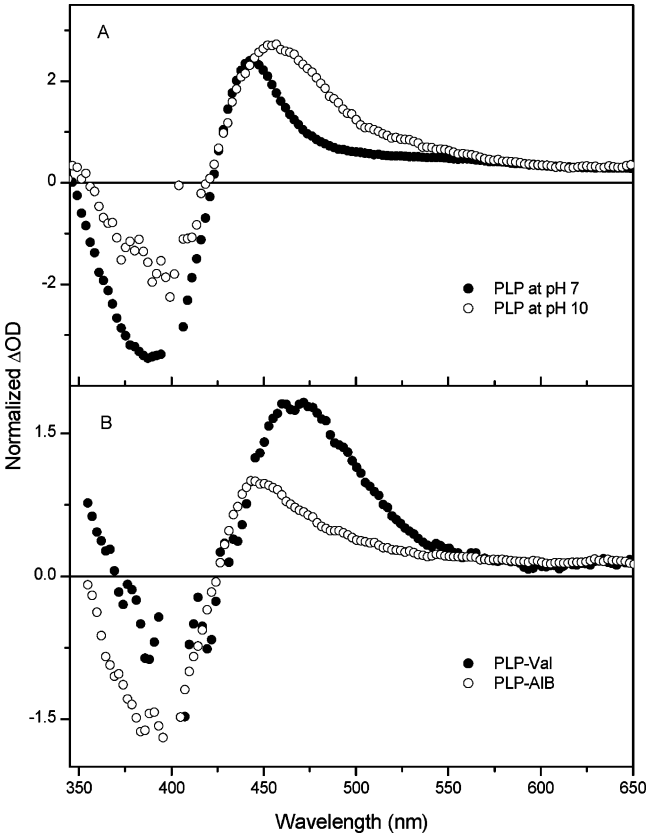

Figure 7. Transient absorption spectra at 7 ns of (A) PLP in H_2O at pH 7.0 (●) and at pH 10.0 (○) and (B) PLP Schiff base in pH 7.0 H_2O with valine (●) and with AIB (○). Spectra normalized to red-wavelength tail.

Cook and co-workers previously postulated excitation of different tautomers based on excitation wavelength.[9] Their study suggested that photoexcitation at 350 nm of the PLP-valine Schiff base in H_2O results in a slow tautomerization of the hydroxyl proton (enolimine) to the nearby Schiff base nitrogen (ketoenamine) before an eventual deprotonation to form a dipolar species. They further demonstrated that the enolimine tautomer could be circumvented by changing the excitation wavelength to 412 nm to excite only the ketoenamine tautomer with subsequent formation of the dipolar species.

Since the different tautomeric forms of PLP-Schiff bases exhibit different absorption properties, the transient signals measured with different photoexcitation wavelengths can be contrasted to identify the dynamics for the different tautomers. Photoexcitation of the PLP-valine Schiff base with 350 nm would be expected to preferentially excite the enolimine tautomer (with its max absorption at 330 nm). However, in comparing those excited-state dynamics with the 400 nm signals, there was no clear dependence on excitation wavelength (Supporting Information, Figure S2), in strong contrast to the previous study by Cook et al.[9] This suggests that, if it occurs at all, tautomerization occurs rapidly within the 250-fs temporal resolution of the 350-nm data.

To investigate possible ESPT formation of the quinonoid intermediate, the PLP-valine Schiff base was excited in D_2O at pD 7. These transient absorption signals revealed appreciably slower kinetics than that in H_2O at pH 7 (Figure 5). This strongly suggests that an ESPT reaction occurs in the PLP-valine Schiff base. Formation of the quinonoid requires removal of the Cα proton, a less labile proton than that in tautomerization. However, D_2O is 2.5 times more basic when compared with H_2O;[28,29] therefore, an ESPT of a less labile proton will be

efficiently replaced with a deuteron. This is also illustrated in the time constants associated with quinonoid formation (Table 1). The dynamics associated with the isotope effect is, for the most part, longer because of the heavier nature of D_2O; however, the second time constant (τ_2) is slightly faster in D_2O than in H_2O as a result of this increased basicity of D_2O facilitating the ESPT.

To confirm further that this ESPT is quinonoid formation, AIB was used to form the Schiff base since it has a methyl group in place of the Cα proton (Figure 1). Transient absorption studies comparing PLP-AIB in H_2O and D_2O at pH/pD 7 with the same excitation wavelength revealed little differences in the kinetic traces (Figure 6).

The PLP-valine Schiff base data was fit to a sequential four-compartment model with longer time constants using global analysis (Table 1). The first time constant represents solvation dynamics. Triplet state formation from a PLP-Schiff base has not been previously reported and is presumably generated in a lower yield than for free PLP because of the significantly longer-lived singlet excited-state population (~1 ns vs 20 ps). Moreover, the dissimilarity of the 8-ns spectrum for the triplet state of PLP at pH 7.0 and the long-lived intermediate in the PLP-valine Schiff base (particularly at wavelengths shorter than 525 nm) suggest that the photoproduct for the Schiff base is not likely a triplet state (Figure 7). Although the PLP pH 10 triplet spectrum shows a striking likeness to the PLP-valine terminal spectrum, the excited-state quenching dynamics is notably longer (Figures 3 and 5, Table 1), indicative of the differing mechanisms for their generation.

The extracted SADS for PLP-valine in H_2O and D_2O show distinctive differences in their stimulated emission bands at wavelengths longer than 500 nm. Those observed in the H_2O samples are much broader than those observed in the D_2O samples (Figure 5). This has been reproduced numerous times and is seen in both AIB and other Schiff base complexes. Since the absorption and fluorescence spectra exhibit a negligible deuterium dependence on their spectral properties, the observed difference in the transient absorption must be attributed to the overlapping excited-state absorption spectra. Clearly, the high-lying excited electronic states couple to vibrations involving significant hydrogen motion.

4. Concluding Comments

Here, the first femtosecond study of the excited-state dynamics of PLP and PLP-Schiff bases in solution is reported. When PLP is photoexcited, rapid solvation dynamics is observed as a red-shifting of the stimulated emission band followed by evolution through two possible routes: (1) intersystem crossing into a long-lived reactive triplet state ($\tau = 150$ ps) or (2) internal conversion to a second excited state that branches between internal conversion to ground state ($\tau = 19$ ps) and intersystem crossing into the triplet state. This triplet state may react to form photoproducts consistent with previous photodegradation studies of PLP. We find that the rate of internal conversion varies depending on the solvent environment with protonation altering the electronic structure of the chromophore and excited-state kinetics of PLP.

When the PLP-valine Schiff base in pH 7.0 water is photoexcited, it tautomerizes within 250 fs and then proceeds through the transamination half-reaction, producing the key intermediate in all PLP-dependent reactions, the carbanionic quinonoid species. This assignment is supported by: (1) PMP formation, (2) peak absorption wavelength at 470 nm (in agreement with the reported absorption max for quinonoid[12]), and (3) slower kinetics in D_2O supporting ESPT. Formation of the quinonoid intermediate through ESPT deprotonation of Cα is corroborated by the observation that its formation is not observed when AIB, an α-methyl amino acid, replaces valine as the substrate. Consequently, we conclude that the increase in enzymatic activity upon photoexcitation observed by Fraiken et al.[4] resulted from rapid formation of the quinonoid intermediate due to excitation of the ketoenamine tautomer. Direct, rapid formation of the central quinonoid intermediate upon photoexcitation can therefore be used to explore the dynamics of PLP-dependent enzymatic reactions with rapid time-resolved spectroscopic techniques, which is a topic of further interest.

Acknowledgment. This work was supported by startup funds from the University of California and with a Career Development Award from the Human Frontiers Science Organization (to D.S.L.) and from a grant (GM54779) from the National Institutes of Health (to M.D.T.). We thank Dorte Madsen for laboratory assistance and constructive discussions.

Supporting Information Available: Absorbance and fluorescence spectra of PLP and PLP-valine (Figure S1). Dynamics of the PLP-valine Schiff base as a function of excitation wavelength demonstrating no variation in the 350-nm pump compared with that of the 400-nm pump (Figure S2). This material is available free of charge via the Internet at http://pubs.acs.org.

References and Notes

(1) Morozov, Y. V. Spectroscopic Properties, Electronic Structure and Photochemical Behavior of Vitamin B6 and Analogs. In *Vitamin B6 Pyridoxal Phosphate: Chemical, Biochemical, and Medical Aspects;* Dolphin, D., Poulson, R., Avramovic, O., Eds.; Wiley & Sons: New York, 1986; Vol. 1A, p 132.

(2) John, R. A. *Biochim. Biophys. Acta* **1995**, *1248*, 81.

(3) Kallen, R. G.; Korpela, T.; Martell, A. E.; Matsushima, Y.; Metzler, C. M.; Metzler, D. E.; Morozov, Y. V.; Ralston, I. M.; Savin, F. A.; Torchinsky, Y. M.; Ueno, H. Chemical and Spectroscopic Properties of Pyridoxal and Pyridoamine Phosphates. In *Transaminases;* Christian, P., Metzler, D. E., Eds.; Wiley & Sons: New York, 1985.

(4) Fraikin, G. Y.; Strakhovskaya, M. G.; Ivanova, E. V.; Rubin, A. B. *Photochem. Photobiol.* **1989**, *49*, 475.

(5) Cornish, T. J.; Ledbetter, J. W. *IEEE J. Quantum Electron.* **1984**, *20*, 1375.

(6) Sage, J. T.; Morikis, D.; Champion, P. M. *Biochemistry* **1991**, *30*, 1227.

(7) Walker, L. A.; Jarrett, J. T.; Anderson, N. A.; Pullen, S. H.; Matthews, R. G.; Sension, R. J. *J. Am. Chem. Soc.* **1998**, *120*, 3597.

(8) Bazhulina, N. P.; Kirpichnikov, M. P.; Morozov, Y. V.; Savin, F. A.; Sinyavina, L. B.; Florentiev, V. L. *Mol. Photochem.* **1974**, *6*, 367.

(9) Benci, S.; Vaccari, S.; Mozzarelli, A.; Cook, P. F. *Biochim. Biophys. Acta* **1999**, *1429*, 317.

(10) Harris, C. M.; Johnson, R. J.; Metzler, D. E. *Biochim. Biophys. Acta* **1976**, *421*, 181.

(11) Ledbetter, J. W.; Askins, H. W.; Hartman, R. S. *J. Am. Chem. Soc.* **1979**, *101*, 4284.

(12) Metzler, C. M.; Harris, A. G.; Metzler, D. E. *Biochemistry* **1988**, *27*, 4923.

(13) Metzler, D. E. *Adv. Enzymol. Relat. Areas Mol. Biol.* **1979**, *50*, 1.

(14) Morrison, A. L.; Long, R. F. *J. Chem. Soc.* **1958**, 211.

(15) Carroll, E. C.; Compton, O. C.; Madsen, D.; Osterloh, F. E.; Larsen, D. S. *J. Phys. Chem. C* **2008**, *112*, 2394.

(16) Kovalenko, S. A.; Dobryakov, A. L.; Ruthmann, J.; Ernsting, N. P. *Phys. Rev. A: At., Mol., Opt. Phys.* **1999**, *59*, 2369.

(17) Cornish, T. J.; Ledbetter, J. W. *Photochem. Photobiol.* **1985**, *41*, 15.

(18) Kurauchi, Y.; Ohga, K.; Morita, S.; Nagamura, T.; Matsuo, T. *Chem. Lett.* **1983**, 349.

(19) Kurauchi, Y.; Ohga, K.; Yokoyama, A.; Morita, S. *Agric. Biol. Chem.* **1980**, *44*, 2499.

(20) Bridges, J. W.; Davies, D. S.; Williams, R. T. *Biochem. J.* **1966**, *98*, 451.

(21) van Stokkum, I. H. M.; Larsen, D. S.; van Grondelle, R. *Biochim. Biophys. Acta* **2004**, *1658*, 262.

(22) Holzwarth, A. R. Data Analysis in Time-Resolved Measurements. In *Biophysical Techniques in Photosynthesis;* Amesz, J., Hoff, A. J., Eds.; Kluwer: Dordrecht, The Netherlands, 1996.
(23) Jimenez, R.; Fleming, G. R.; Kumar, P. V.; Maroncelli, M. *Nature* **1994**, *369*, 471.
(24) Larsen, D. S.; Vengris, M.; van Stokkum, I. H. M.; van der Horst, M.; Cordfunke, R.; Hellingwerf, K. J.; van Grondelle, R. *Chem. Phys. Lett.* **2003**, *369*, 563.
(25) Morozov, Y. V.; Cherkashina, L. P. *Mol. Photochem.* **1977**, *8*, 45.
(26) Goncalves, P. J.; De Boni, L.; Neto, N. M. B.; Rodrigues, J. J.; Zilio, S. C.; Borissevitch, I. E. *Chem. Phys. Lett.* **2005**, *407*, 236.
(27) Walters, L. S.; Cornish, T. J.; Askins, H. W.; Ledbetter, J. W. *Anal. Biochem.* **1982**, *127*, 361.
(28) Dahlberg, D. B.; Long, F. A. *J. Am. Chem. Soc.* **1973**, *95*, 3825.
(29) Hibbert, F.; Long, F. A. *J. Am. Chem. Soc.* **1971**, *93*, 2836.